DOI: 10.1021/ma900446e

Macromolecules
COMMUNICATION TO THE EDITOR

Shear Effect on Crystallizing Single Wall Carbon Nanotube/Poly(butylene terephthalate) Nanocomposites

J. J. Hernández, M. C. García-Gutiérrez, A. Nogales, D. R. Rueda, and T. A. Ezquerra*

Instituto de Estructura de la Materia, CSIC, Serrano 119, 28006 Madrid, Spain

Received February 27, 2009
Revised Manuscript Received May 11, 2009

Because of their mechanical properties, carbon nanotubes (CNT) are promising reinforcing additives for a new generation of nanocomposite materials.[1,2] The homogenization of the nanotube dispersion within the polymer matrix at the nanometer scale is a crucial step in order to gain full benefit of the reinforcing power of carbon nanotubes.[3] In general, typical polymer nanocomposite processing involves solidification, either by crystallization or by vitrification, from a molten state distorted by a combination of shear and elongational flow fields. The effect of flow fields on the nanostructure of polymers and nanocomposites has a strong impact on their physical properties.[4−7] In particular, shear fields applied to polymer composite materials may affect the nucleation density of the polymer matrix,[8,9] the orientation of the nanoadditive network,[10] or the orientation of the polymer matrix,[9] among others. Recent experiments have shown that carbon nanotubes are very efficient in templating oriented polymer crystal growth.[11−14] In general, it is known that the carbon nanotube surface imposes to polymer crystals a growth direction perpendicular to the nanotube longitudinal axis. Because of the efficiency of carbon nanotubes as nucleating agents,[15] it seems very difficult to either control or modify this characteristic perpendicular orientation of lamellar polymer crystals. In general, hot-pressed films of CNT nanocomposites exhibit a preferred orientation of the CNTs perpendicular to the pressing direction. This effect has been reported by Haggenmueller et al. for SWCNT/polyethylene composites[12] and by García-Gutiérrez et al. for SWCNT/PBT composites.[9] Thus, the CNT orientation dictates the orientation of polymer chains templating polymer crystallization in such a way that lamellae grow perpendicular from the SWCNT surface.[9,12] The effectiveness of the templating effect of SWCNT makes difficult obtaining other morphologies in hot-pressed SWCNT nanocomposites like for example crystal lamellae parallel to the SWCNT surface and therefore parallel to the film surface. In this Communication we show how, by applying a shear step to a crystallizing nanocomposite based on poly(butylene terephthalate) (PBT) ($M_w \approx 15\,000$ g/mol) and oxidized single wall carbon nanotubes (SWCNT) (from CNI Technology Co., Houston, TX, synthesized by using the HiPco method), the final orientation of the polymer matrix can be controlled.

The SWCNT/PBT nanocomposite was prepared by "in situ" polymerization as described elsewhere.[16] The nanocomposite was extruded from the reactor by compressed nitrogen, and subsequently it was pelletized and injection-molded with a Baby Plast, Model 6/10 (Cronoplast S.L. Comp) injection molding machine into long pieces with a rectangular cross section of 2×4 mm^2. The injection molding parameters were: injection pressure 25 bar, melt temperature 240−250 °C, mold temperature 40 °C, hold time 6 s and cooling time 20 s. Nanocomposite films of about 0.1 mm thickness were obtained by compression molding at 240 °C for 2 min and subsequently quenched under constant pressure at a cooling rate of ~300 °C min^{-1}. Small-angle X-ray scattering (SAXS) measurements were performed at the ID2 beamline at the European Synchrotron Radiation Facility (ESRF) in Grenoble, France, at wavelength of $\lambda = 0.1$ nm. An X-ray beam parallel to the flat surface of the rotating plates was chosen because it can be advantageous to characterize orientations parallel to the rotating plates. SAXS patterns were recorded by a two-dimensional CCD camera (FReLoN Kodak CCD, with an input field of 100 mm × 100 mm). The sample-to-detector distance was fixed to 2640 mm. Typical beam size at the sample position is 0.1×0.1 mm^2. Data reduction procedure has been previously described.[9] Shear was applied to the sample by using a RS300 (HAAKE) rheometer.[9,17] The rheometer has been modified to accommodate a truncated cone with a radius, $R = 3$ mm, for the smallest circle base. The gap, set to $h = 0.6$ mm, was filled at room temperature with about six films located edge-on to incident X-ray beam. Under these conditions the maximum shear rate applied to the sample is given by $\dot{\gamma} = (R/h)\Omega$, where Ω is the angular speed. Different maximum shear rates, $\dot{\gamma}$, were applied for different times in order to obtain a maximum constant strain of 2000%. In a previous report[9] it was shown that, under quiescent conditions, SWCNT bundles are lying essentially with their main axes parallel to the flat surface of the sample and that PBT exhibits very little orientation effects as compared with those observed in SWCNT/PBT nanocomposites.

We accomplished two types of shear experiments as schematically described in Figure 1. In the first case, (a) in Figure 1, a shear step is applied to the polymer for a certain time at a temperature higher than its melting temperature, T_m. After cessation of the shear the sample is immediately cooled down to the crystallization temperature, T_c, and the structural evolution with time was followed by SAXS. We will refer to this case of application of shear above the melting temperature as SMT. In the second case, (b) in Figure 1, the shear is applied when the sample reaches T_c by cooling from the melt. We will refer to this case of application of shear at the crystallization temperature as SCT. Two-dimensional SAXS images were taken immediately after the polymer reached a temperature $T_c = 208$ °C. The data acquisition time for each SAXS pattern was typically 0.1 s. The scattering patterns were azimuthally integrated in order to obtain the one-dimensional scattering intensity as a function of the scattering vector q. A further integration in the q range of the scattered intensity allows one to define the total integrated intensity. This magnitude, represented as a function of time, can be used to characterize the crystallization kinetics. Nevertheless, in order to compare different crystallization kinetics, the use of relative integrated intensity values is recommended. The latter ones are derived by subtracting the first integrated intensity value from all of them, the resulting data being normalized to the final value of the crystallization process. The oriented fraction parameter, Φ, was obtained empirically on the basis of an experimental strategy developed for PBT,[6,9] and it is explained in the legend of Figure 2. Additionally, the Hermans orientation function was also estimated.[9,18] Previous quiescent crystallization experiments performed in a great variety of polymers[12−14] have shown that carbon nanotubes template anisotropic crystallization in which crystalline lamellae tend to grow perpendicular to

*To whom correspondence should be addressed.

 Published on Web 06/09/2009

nanotube surface. The application of a shear step above the melting temperature (SMT) does not vary significantly this crystallization scenario, although increases the fraction of oriented material in the polymer.[9] In Figure 3 it is shown that the application of the shear step at a given crystallization temperature (SCT) can change substantially the growth pattern in relation to that observed for the SMT procedure by counterbalancing the templating effect of the carbon nanotubes. Figure 3 compares a series of SAXS patterns corresponding to the crystallization of a SWCNT/PBT nanocomposite (0.2 wt % of SWCNT) at T_c = 208 °C under SMT (Figure 3a) and SCT (Figure 3b) conditions. For the last case, the application of the step shear (20 s^{-1}) is indicated in the figure by an arrow. The time dependence of the relative integrated SAXS intensity, the oriented fraction parameter, Φ, and the Hermans orientation function, f_2, is shown in Figure 4. The moment at which the step shear was applied under SCT conditions has been indicated by an arrow on the time axis. The kinetics of crystallization becomes slightly faster under SCT conditions (Figure 4a). This can be understood, according to previous reports,[6,9] as due to a faster relaxation of shear-induced nuclei at higher temperature than at lower ones. Under SMT conditions the oriented fraction tends to increases as crystallization proceeds (Figure 4b). The sample starts with negative values of the orientation function (Figure 4c) but soon evolves toward positive values. This is characteristic of initial SAXS patterns with an excess of scattered intensity in the equatorial region which can be attributed to the scattering of the carbon nanotubes located preferentially with their main axis parallel to the shear direction.[9] At the end of the crystallization process, SAXS patterns exhibit an excess of scattering concentrated in the meridian part (see Figure 3a), indicating that a certain amount of crystalline lamellae have grown perpendicular to the shear direction. This effect was previously interpreted assuming that carbon nanotubes act as heterogeneous nuclei providing surfaces over which oriented PBT crystals can grow.[9] This mechanism has been referred to as size-dependent soft epitaxy.[19] However, the situation dramatically changes for the SCT experiments. As shown in Figure 3, the final SAXS patterns taken at the end of the crystallization are completely different for the two shear conditions. For SCT conditions, data of Figure 4c clearly indicate a change from positive to negative of the Hermans orientation function upon application of shear. This effect indicates that in

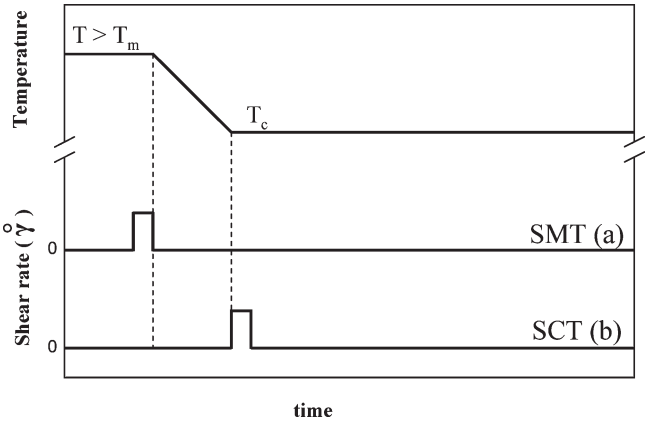

Figure 1. Schematic description of the two types of shear experiments. In (a) the sample, after reaching the melting temperature, T_m, is subjected to a shear step for a certain time. After shear cessation the sample is cooled down to the crystallization temperature, T_c (SMT procedure). In (b) the molten sample is first cooled down to T_c. Subsequently, a shear step is applied for a certain time (SCT procedure).

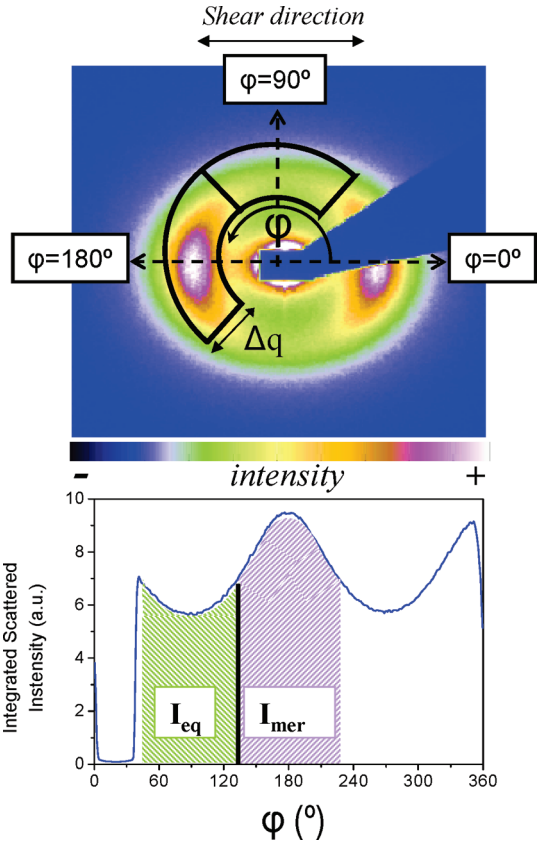

Figure 2. Strategy to estimate the oriented fraction parameter Φ. The 2D SAXS pattern (a) is divided into two quadrants centered along the meridian (0°−180° line) and the equator (90°−270° line). A cake, represented by the continuous lines in (a), is defined in each quadrant with a width of Δq = 20 nm^{-1}, where q is the scattering vector $q = 4\pi\lambda^{-1}$ sin θ, and 2θ is the scattering angle. The cakes are centered at the q values corresponding to the maximum scattered intensity. The scattered intensity is radial integrated within the cakes and represented as a function of the azimuth angle φ (b). A second integration in φ is done in order to define the magnitudes I_{mer} and I_{eq} for the meridian and equator regions, respectively (shadowed regions). An empirical oriented fraction parameter is defined by means of $\Phi = (I_{mer} - I_{eq})/(I_{mer} + I_{eq})$.

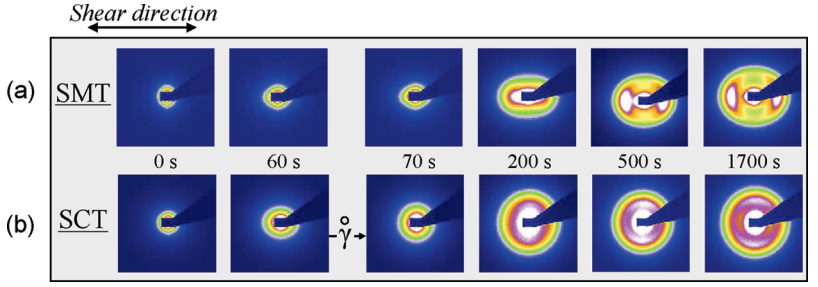

Figure 3. SAXS patterns corresponding to the crystallization of a SWCNT/PBT nanocomposite with 0.2 wt % of SWCNT at T_c = 208 °C under (a) SMT conditions and (b) SCT conditions. In both cases with a shear rate of 20 s^{-1}.

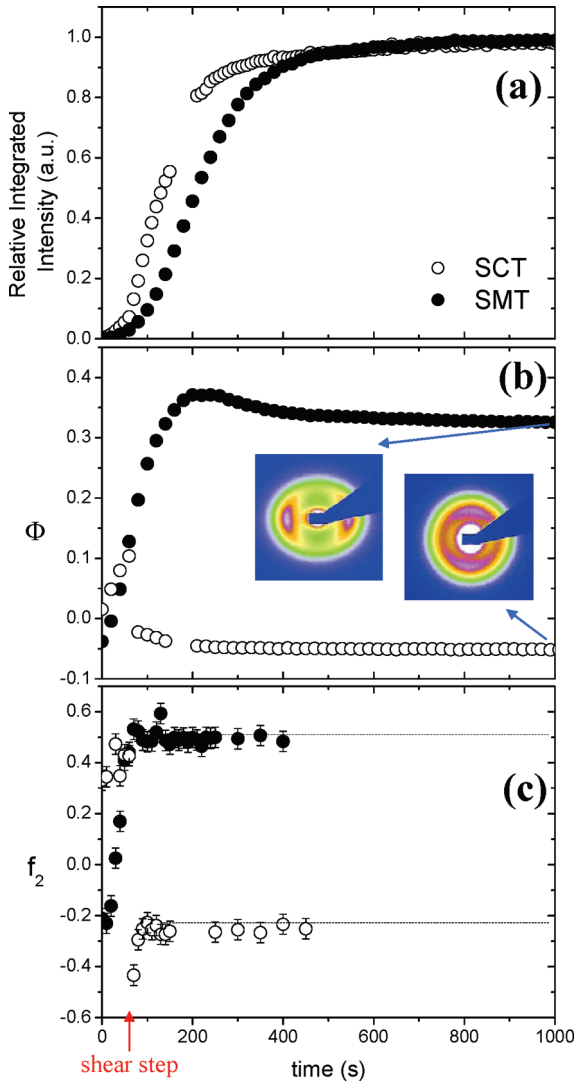

Figure 4. (a) SAXS relative integrated intensity, (b) oriented fraction, and (c) Hermans orientation function for a SWCNT/PBT nanocomposite with 0.2 wt % of SWCNT at T_c = 208 °C, in both SMT (●) and SCT (○) conditions with a shear rate of 20 s^{-1}. The application of a shear step for SCT conditions has been indicated by an arrow in the time axis.

the initial crystallization stages, before the application of the shear step, crystalline lamellae tend to grow perpendicular to the film surface. The higher f_2 value before shear under SCT conditions indicates a higher scattered intensity concentrated in the meridian and therefore a higher amount of crystal lamella due to a faster crystallization kinetics. The application of the shear step dramatically changes this trend almost changing the crystal growth direction by 90°. This effect is also reflected in the oriented fraction parameter values (Figure 4b). Before shear, under SCT conditions, there is a scattering increase in the meridian sector. After shearing the oriented fraction parameter reverses because the SAXS patterns exhibit a concentration of the scattering in the equatorial sector. The experiments illustrated in Figures 3 and 4 indicate that the morphology consisting on PBT crystalline lamellae perpendicular to the shear direction is not the only possible in carbon nanotubes nanocomposites. By applying a shear step to the crystallizing system at a given crystallization temperature (SCT conditions, Figure 1b), a dramatic change of the final orientation is obtained as compared to that observed for the SMT conditions.[9] The initial positive Hermans orientation function, before shearing, suddenly turns into a negative value once the shear step is applied. This negative value indicates an orthogonal change in the lamellar crystal growth upon application of shearing. The Hermans orientation function takes a value of 1 when the scattered intensity is concentrated in the meridian. Even under SMT conditions the final f_2 value is far from this limit, indicating a certain contribution from isotropic crystallization. In a first approach we attribute the increase of f_2 after shear under SCT conditions to a background of isotropic scattering. As a matter of fact, the final scattering pattern shown in the inset of Figure 4b exhibits significant isotropic scattering in the equatorial region. Considering that in the case presented here shear is applied over a crystallizing melt, we propose that upon shearing some grown lamellae could be disposed parallel to the shear direction inducing subsequent crystallization to be templated by these lamellar crystals rather than by the carbon nanotubes. These experiments emphasize the variety of crystalline microstructures which may appear in carbon nanotube/polymer nanocomposites upon processing when a complex combination of force fields and temperature gradients are active.

Acknowledgment. The authors thank the financial support from the CAM/CSIC (CCG07-CSIC/MAT-2296) and from MAT2005-01768 (MICINN), Spain, for generous support of this investigation. M.C.G.-G. is grateful to the Ramón y Cajal Program for the support of this research. J.J.H. thanks the Spanish Ministry for Science and Innovation (MICINN) for the tenure of a fellowship. The technical assistance of P. Panine during measurement in ID2 at ESRF is grateful acknowledged.

References and Notes

(1) Moniruzzaman, M.; Winey, K. I. *Macromolecules* **2006**, *39*, 5194.
(2) Vaia, R. A.; Wagner, H. D. *Mater. Today* **2004**, November, 32.
(3) Schaefer, D. W.; Justice, R. S. *Macromolecules* **2007**, *40*, 8501.
(4) Somani, R. H.; Hsiao, B. S.; Nogales, A.; Srinivas, S.; Tsou, A. H.; Sics, I.; Balta-Calleja, F. J.; Ezquerra, T. A. *Macromolecules* **2000**, *33*, 9385.
(5) Seki, M.; Thurman, D. W.; Oberhauser, J. P.; Kornfield, J. A. *Macromolecules* **2002**, *35*, 2583.
(6) Li, L.; de Jeu, W. H. *Macromolecules* **2004**, *37*, 5646.
(7) Heeley, E. L.; Fernyhough, C. M.; Graham, R. S.; Olmsted, P. D.; Inkson, N. J.; Embery, J.; Groves, D. J.; McLeish, T. C. B.; Morgovan, A. C.; Meneau, F.; Bras, W.; Ryan, A. J. *Macromolecules* **2006**, *39*, 5058.
(8) Byelov, D.; Panine, P.; Remerie, K.; Biemond, E.; Alfonso, G. C.; de Jeu, W. H. *Polymer* **2008**, *49*, 3076.
(9) García-Gutiérrez, M. C.; Hernández, J. J.; Nogales, A.; Panine, P.; Rueda, D. R.; Ezquerra, T. A. *Macromolecules* **2008**, *41*, 844.
(10) Xu, D.; Wang, Z.; Douglas, J. F. *Macromolecules* **2008**, *41*, 815.
(11) Li, C. Y.; Li, L.; Cai, W.; Kodjie, S. L.; Tenneti, K. K. *Adv. Mater.* **2005**, *17*, 1198.
(12) Haggenmueller, R.; Fischer, J. E.; Winey, K. I. *Macromolecules* **2006**, *39*, 2964.
(13) Minus, M. L.; Chae, H. G.; Kumar, S. *Polymer* **2006**, *47*, 3705.
(14) García-Gutiérrez, M. C.; Nogales, A.; Rueda, D. R.; Domingo, C.; García-Ramos, J. V.; Broza, G.; Roslaniec, Z.; Schulte, K.; Ezquerra, T. A. *Compos. Sci. Technol.* **2007**, *67*, 798.
(15) Bhattacharyya, A. R.; Sreekumar, T. V.; Liu, T.; Kumar, S.; Ericson, L. M.; Hauge, R. H.; Smalley, R. E. *Polymer* **2003**, *44*, 2373.
(16) Broza, G.; Kwiatkowska, M.; Roslaniec, Z.; Schulte, K. *Polymer* **2005**, *46*, 5860.
(17) Panine, P.; Gradzielski, M.; Narayanan, T. *Rev. Sci. Instrum.* **2003**, *74*, 2451.
(18) Prasad, A.; Shroff, R.; Rane, S.; Beaucage, G. *Polymer* **2001**, *42*, 3103.
(19) Li, L.; Li, B.; Hood, M. A.; Li, C. Y. *Polymer* **2009**, *50*, 953.